Supplementary Information for

Laser-drilled functional wood materials show improved dimensional stability upon humidity changes - a neutron imaging analysis

Yong Ding [1 2 # *], Mahdieh Shakoorioskooie [3 #], David Mannes [3], Zhidong Zhang [4], Dmitry Chernyshov [5], Ingo Burgert [1, 2]

[1] Wood Materials Science, Institute for Building Materials, ETH Zürich, 8093, Zürich, Switzerland.

[2] WoodTec Group, Cellulose & Wood Materials, Empa, 8600 Dübendorf, Switzerland

[3] Laboratory for Neutron Scattering and Imaging, PSI Center for Neutron and Muon Sciences, Forschungsstrasse 111, 5232 Villigen, PSI, Switzerland

[4] Durability of Engineering Materials, Institute for Building Materials, ETH Zurich, 8093 Zurich, Switzerland

[5] Swiss-Norwegian Beam Lines at European Synchrotron Radiation Facility, 71 Avenue des Martyrs, Grenoble 38043, France

[#] Contribute equally

* Corresponding to yoding@ethz.ch

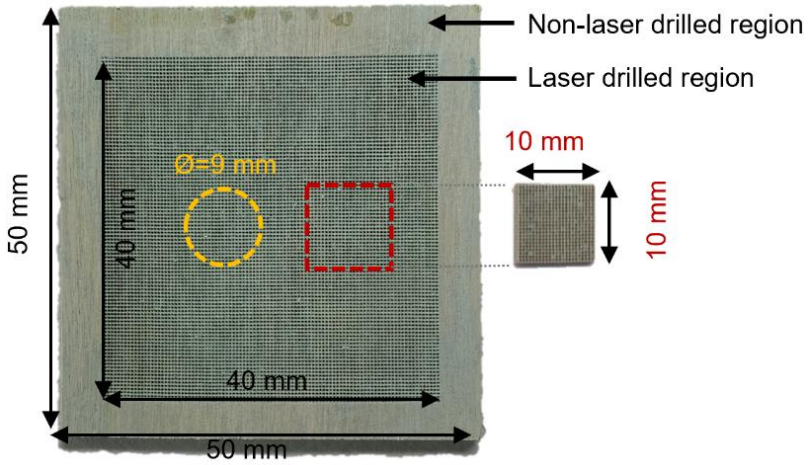

Figure S1. Image of MOF/wood sample with the original sample dimension (50mm×50mm×1.5mm). Round disks with a diameter of 9 mm were cut for neutron imaging analysis (marked in yellow). Specimens with a dimension of 10mm×10mm×1.5mm were cut out and used for MOF loading calculation and density (marked in red).

Humidity logs for the GR-1 and GR-2 measurements

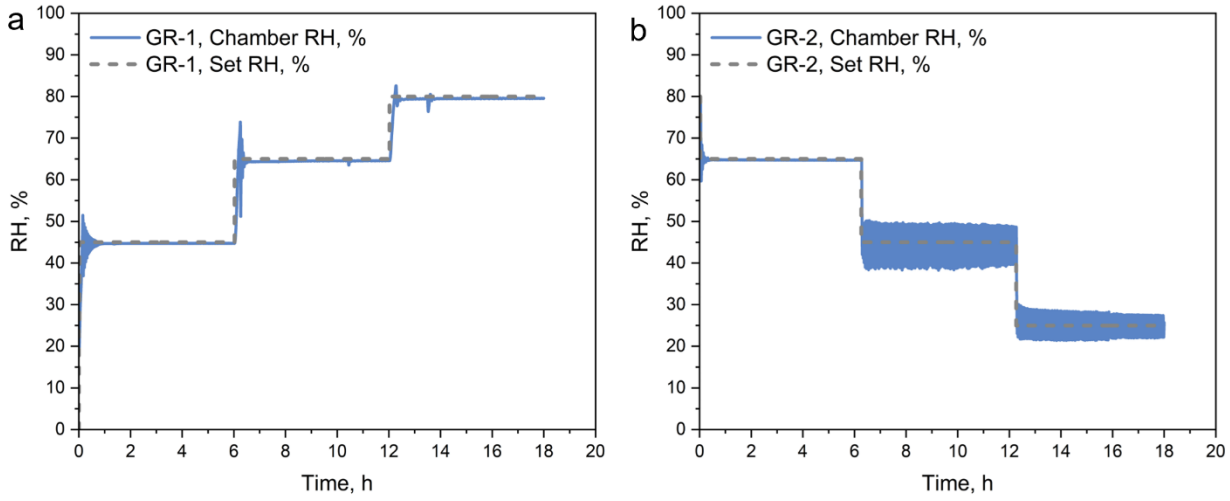

Figure S2. The set-R.H. and real R.H. during GR-1 and GR-2.

Tomogram reconstruction and optimization for Golden Ratio tomography

The imaging sequence included the acquisition of dark-current (DC) and open-beam (OB) radiographs at the outset, essential for the normalization of the radiographs. To further refine the imaging process of the O-tomography and account for neutron scattering, black-body (BB) radiographs were also obtained. This involved the use of a 5-mm thick aluminum frame including a 10 × 10 grid of cylindrical Ø0.5 mm inserts (*black bodies*) made of $^{10}B_4C$. The arrangement of these black bodies allowed for precise evaluation and correction of scattering effects, ensuring the clarity and accuracy of the neutron radiographs (Carminati et al., 2019).

Determining the optimal number of projections required for GR reconstruction under varying R.H. conditions was a critical step of the methodology. Given the continuous acquisition of projections throughout the entire R.H. variation and conditioning, each projection was acquired with an exposure time of 35 seconds. To ascertain the number of projections necessary to reconstruct a tomogram with an acceptable signal-to-noise ratio (SNR), we conducted a series of GR reconstructions, varying the number of projections for one sample and analyzing the SNR of the resulting tomograms. The analysis, illustrated in **Figure S3a**, demonstrates that the SNR of the GR reconstructions (tested on the MOF/wood composite sample) increased sharply with the initial addition of projections but eventually reached a semi-plateau, indicating diminishing returns on the SNR improvement with additional projections. Based on this observation, we selected 130 projections as the optimal number for the reconstructions. This optimization was substantiated by the temporal evolution of histograms from the MOF/wood composite sample reconstructed with this optimal number, which confirmed the capture of variations on the high-intensity side as expected, associated with water uptake of the sample (**Figure S3b**). Additionally, the mean temporal average intensity changes further confirmed the feasibility of this setting (**Figure S3c**). With this optimized configuration, we were able to achieve tomographic reconstructions every 80 minutes, resulting in a total of 13 tomograms covering all conditioning steps for each GR-tomography. This reconstruction frequency allowed us to closely monitor the dynamic moisture interactions within the wood samples.

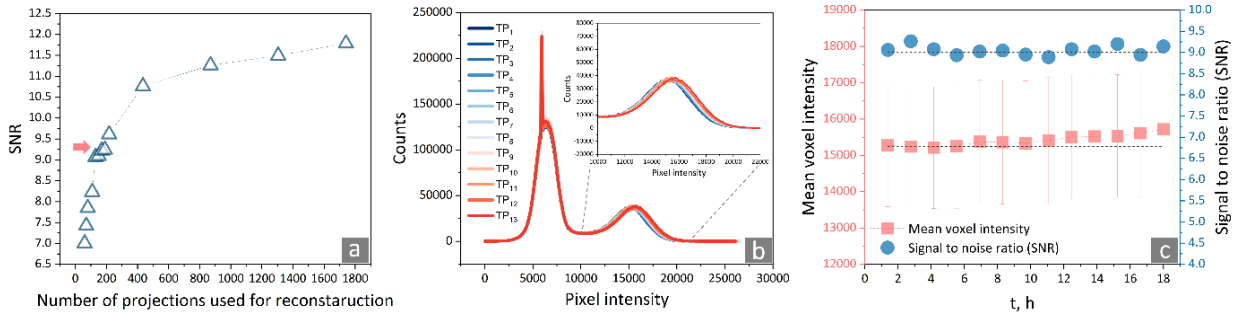

Figure S3 The spatial and temporal optimization results for the golden-ratio (GR) tomography: (a) Variation of the signal-to-noise ratio (SNR) upon increasing the number of projections used for the GR reconstruction; (b) temporal evolution of the histograms of the MOF/wood sample reconstructed with the optimal (selected number of projections from the previous step (a)), with focus on the higher intensity parts of the histogram (indicating uptake of water); and (c) the temporal average intensity changes and the SNR distribution for the same reconstructed time-points in the same sample (as b).

XRD patterns of samples

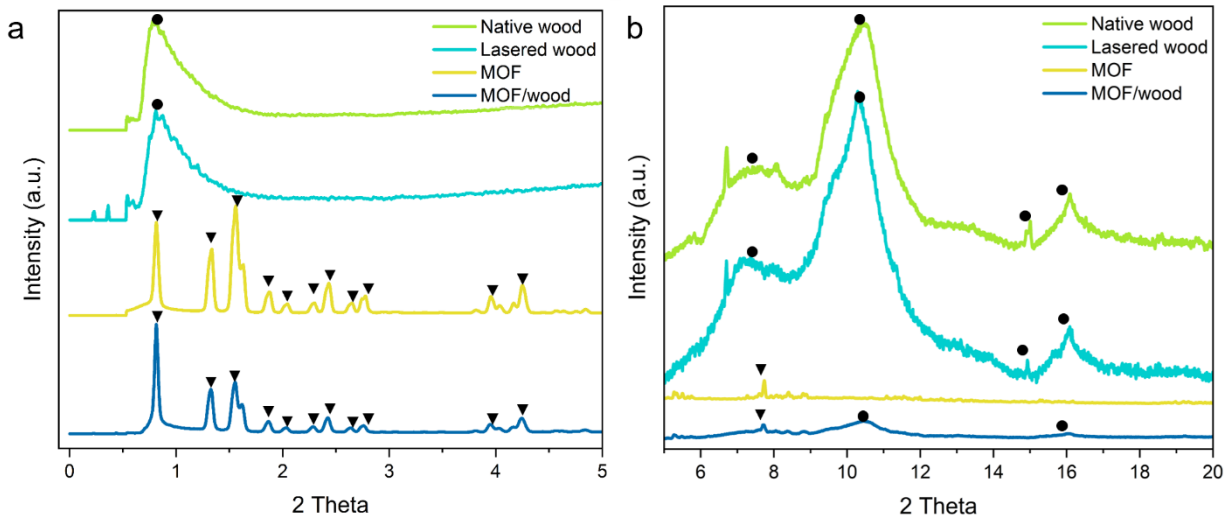

Figure S4. (a-b) XRD patterns of native wood, laser wood, MOF MIL-101(Cr) and MOF/wood composite. The round dots indicate the characteristic peaks of wood, while the rectangular dots indicate the characteristic diffraction peaks of MOF MIL-101(Cr).

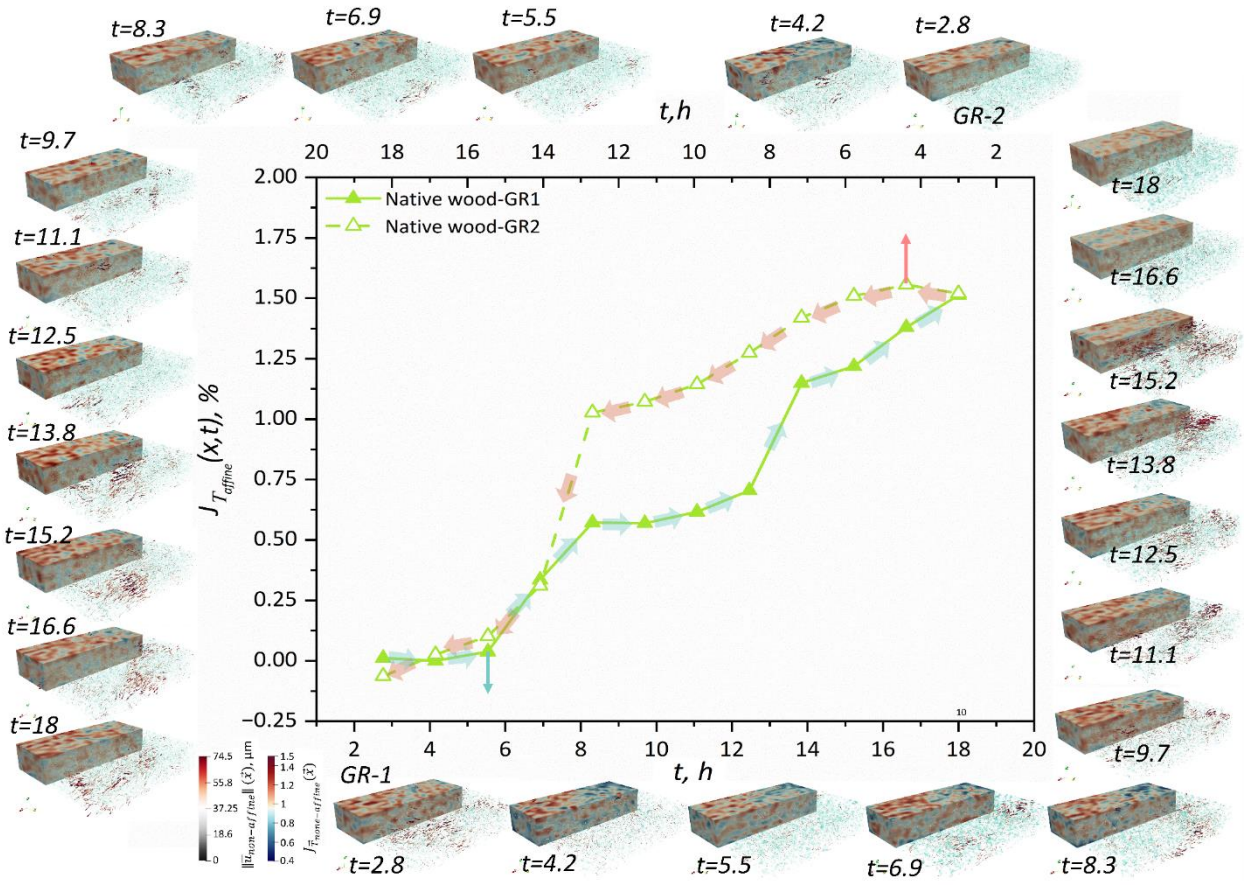

Figure S5. Illustration of the dynamics of volumetric expansion/ shrinkage in native wood during the GR1 and GR2 tomographies, with additional demonstrations of the local deformations and water transport dynamics occurring simultaneously alongside the global volumetric changes, at different time point.

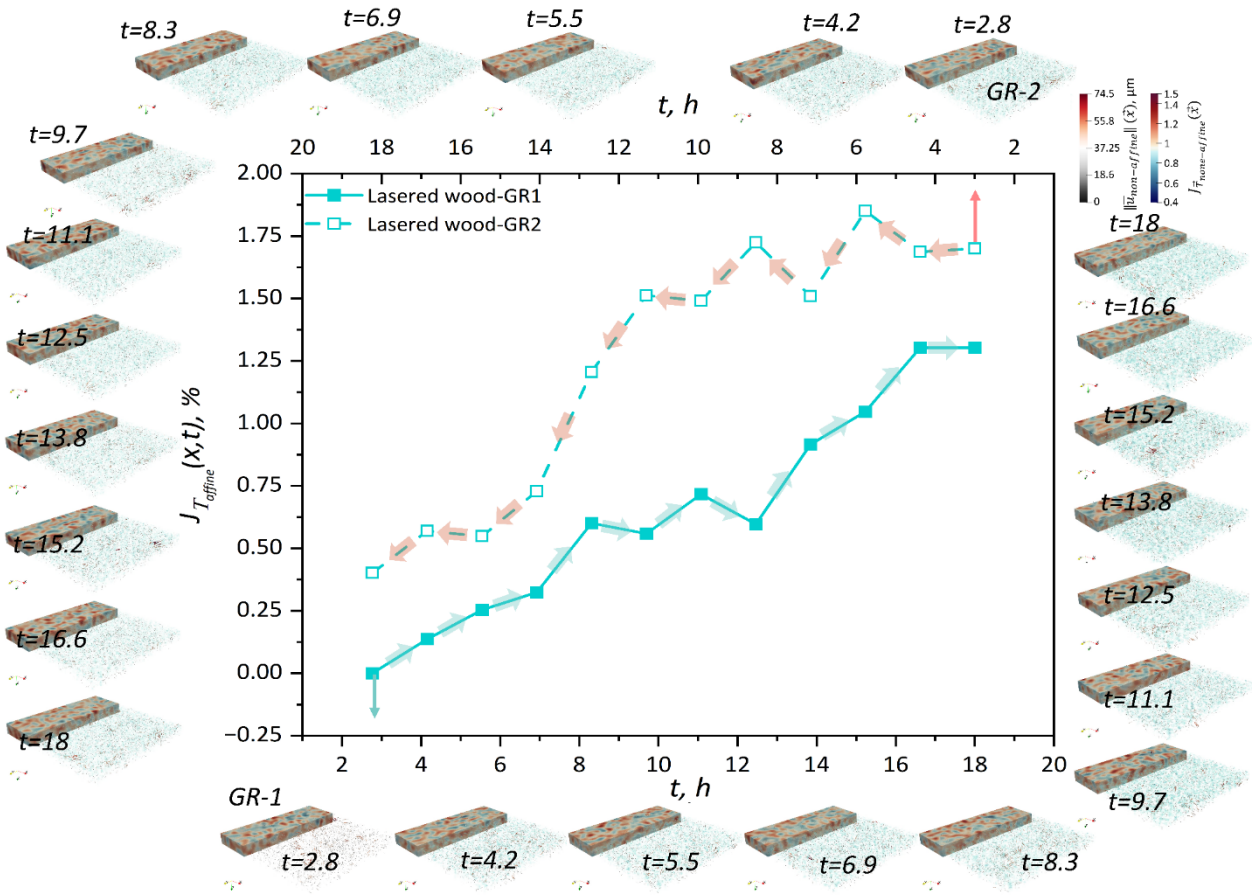

Figure S6. Illustration of the dynamics of volumetric expansion/ shrinkage in lasered wood during the GR1 and GR2 tomographies, with additional demonstrations of the local deformations and water transport dynamics occurring simultaneously alongside the global volumetric changes, at different time point.

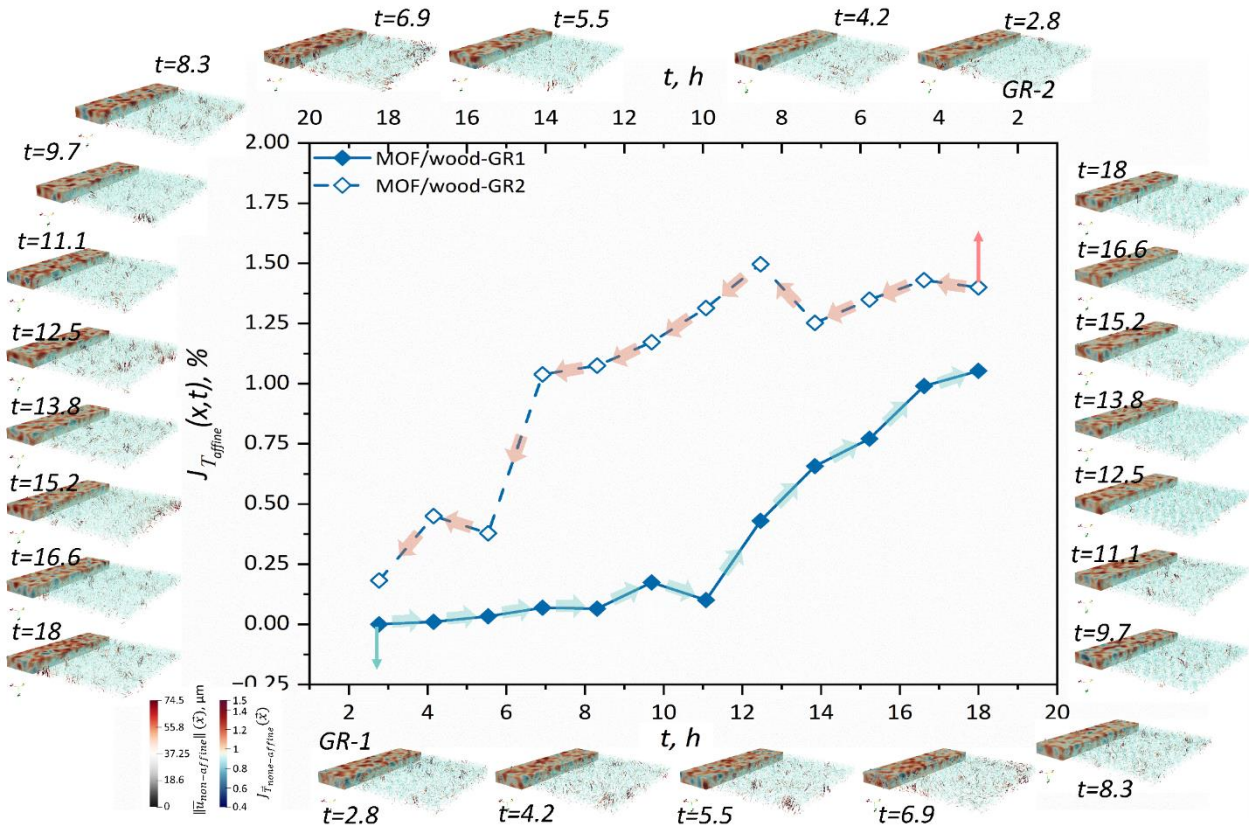

Figure S7. Illustration of the dynamics of volumetric expansion/ shrinkage in MOF/wood during the GR1 and GR2 tomographies, with additional demonstrations of the local deformations and water transport dynamics occurring simultaneously alongside the global volumetric changes, at different time point.

References

Carminati, C., Boillat, P., Schmid, F., Vontobel, P., Hovind, J., Morgano, M., . . . Gruenzweig, C. (2019). Implementation and assessment of the black body bias correction in quantitative neutron imaging. *Plos One,* 14(1), e0210300.